Photopolymerization Behavior of Thiol−Acrylate Monomers in Clay Nanocomposites

Kwame Owusu-Adom,[†] Joel Schall,[‡] and C. Allan Guymon*,[†]

Department of Chemical & Biochemical Engineering, University of Iowa, 4133 Seamans Center, Iowa City, Iowa 52241, and Radiaiton Cure and Anaerobic Technologies Division, Henkel Corporation, 1001 Trout Brook Crossing, Rocky Hill, Connecticut 06067

Received November 26, 2008; Revised Manuscript Received February 18, 2009

ABSTRACT: This study investigates the influence of organoclays modified with polymerizable dispersants on the photopolymerization and physical properties of a binary thiol−acrylate copolymer system. Real-time infrared spectroscopy (RTIR) was used to characterize polymerization behavior, while dynamic mechanical analysis (DMA) and photorheometry were utilized to investigate mechanical and shrinkage properties. Adding nonpolymerizable organically modified clays into thiol−acrylate system leads to no significant changes in photopolymerization rate as compared to the unfilled polymer. Lower thiol conversion but equivalent acrylate conversions as the neat formulation are observed when nonreactive organoclay is added. On the other hand, for organoclays with incorporated acrylate functionalities, higher photopolymerization rates are achieved. As the concentration of acrylated organoclays increase, higher thiol conversion also occurs. The higher polymerization rates are due to reduced termination rates resulting from lower mobility radicals formed on the clay surface. Increases in Young's modulus are observed with addition of nonpolymerizable organoclays, and much higher Young's modulus is obtained with polymerizable organoclays incorporated into the polymer matrices. Polymerization-induced shrinkage is significantly reduced upon incorporating polymerizable organoclay into the photopolymer nanocomposite. An increased tendency toward step-growth polymerizations upon adding thiolated organoclays lead to reduction in shrinkage even with the higher Young's modulus achieved in these nanocomposites.

Introduction

Polymer nanocomposites have been researched over the past decades based on the opportunity to improve physical and thermal properties with incorporation of nanometer-sized particles into polymer hosts. For polymer nanocomposites in which the inorganic filler is clay, additional attraction stems from the relatively low cost and the chemical nature of clay particles. Clay is composed of negatively charged aluminosilicate platelets separated by a van der Waals distance.[1,2] The negative charges are counterbalanced by exchangeable cations embedded between adjacent clay platelets. Because of the hydrophilic nature of the clay, quaternary ammonium surfactants are typically utilized to modify the surface in order to enhance dispersion in organic monomers and/or polymers.

Although clay−polymer nanocomposites have been developed utilizing a number of polymers, their use has been limited primarily to thermally initiated polymer systems or solvent-processed, un-cross-linked polymers. Other polymeric materials, such as photopolymers, which have applications ranging from coatings, thin films, and biological systems,[3−9] could benefit from the unique property enhancements induced by clay nanoparticles. Photopolymerization continues to grow rapidly due to the ultrarapid nature of the reactions, spatial and temporal control of initiation, and temperature-independent initiation. Photopolymers essentially consist of 100% solids and therefore reduce or eliminate the use of solvents and other volatile organic compounds (VOC).[10]

Recent research has demonstrated various clay−photopolymer nanocomposites based on acrylate and epoxy systems.[11−21] These nanocomposites show some improvements in both thermal and mechanical properties without significant changes to the photopolymerization rate when compared to the pristine polymer. However, the improvements are well below those observed in linear polymer systems. Further enhancement to photopolymer nanocomposite materials could be realized from additional understanding of the evolution of their physical properties with respect to reaction behavior. For instance, the large aspect ratio of clay nanoparticles may induce unique photopolymerization behavior that could be explored to optimize polymer nanocomposite properties. Researchers have examined ordering and surface effects and their influence on polymerization behavior.[22] Significantly higher rates of polymerization have been demonstrated in polymerizations performed in various template media.[23] Template polymerizations have also been explored to control polymer morphology in a variety of photopolymerizable systems.[24,25]

In the majority of research pertaining to photopolymerizable systems, including that for nanocomposite systems formed through free radical reactions, (meth)acrylate-based formulations are most commonly used due to availability of monomers and the range of properties that can be designed from those monomers. Unfortunately, the polymerization of (meth)acrylate-based photopolymers are inhibited by atmospheric oxygen, exhibit significant shrinkage, and are often limited by incomplete monomer conversion.[26,27] Photopolymers consisting of thiol monomers copolymerized with other molecules which have terminally unsaturated carbon−carbon double bonds (enes) have recently been investigated as alternatives to (meth)acrylate-based photopolymers.[28−38] Thiol−ene photopolymerization occurs through a step-growth reaction mechanism that leads to more uniform polymer network and reduced shrinkage.[39] On the other hand, these systems typically exhibit reduced mechanical stability due to lower cross-link density of the polymer network. Many advances have been demonstrated that improve mechanical stability by designing specific properties into the monomer backbone. Lee et al., for example, have shown that mechanically stable polymers with reduced shrinkage can be generated from combination of multifunctional allyl ethers and thiols.[37,38] To achieve desired mechanical properties, thiol and ene monomers

* Corresponding author: Ph 319-335-5015; Fax 319-335-1415; e-mail cguymon@engineering.uiowa.edu.
[†] University of Iowa.
[‡] Henkel Corporation.

10.1021/ma802656x CCC: $40.75
Published on Web 04/14/2009

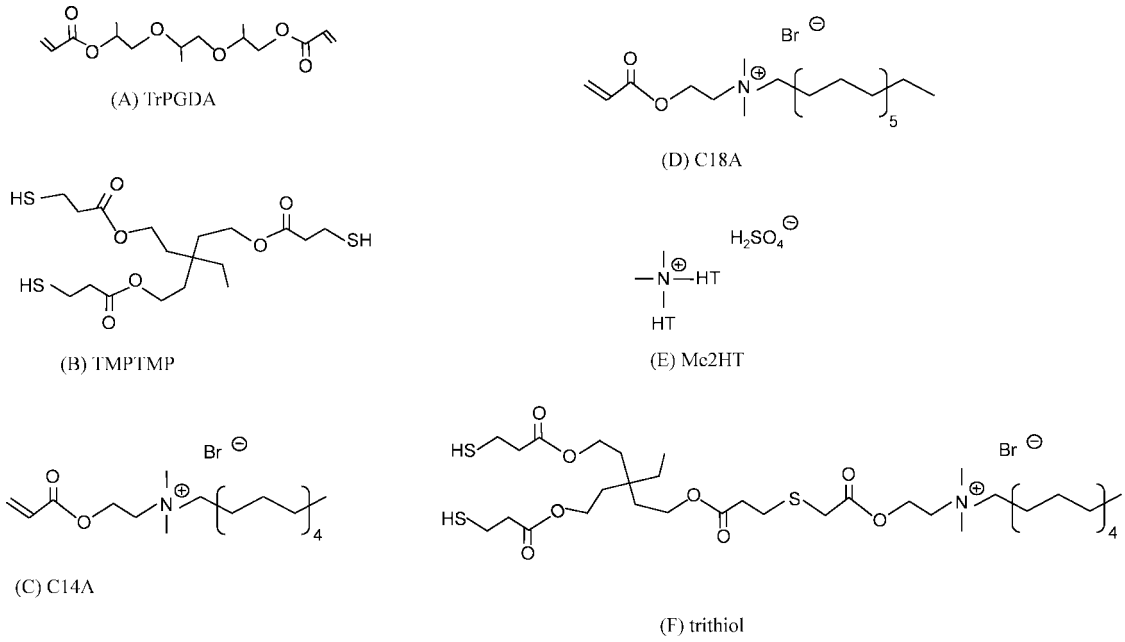

Figure 1. Chemical structures of (A) tripropylene glycol diacrylate (TrPGDA), (B) trimethylolpropane tris(3-mercaptopropionate (TMPTMP), (C) tetradecyl-2-acryloyloxy(ethyl)dimethylammonium bromide (C14A), (D) octadecyl-2-acryloyloxy(ethyl)dimethylammonium bromide (C18A), (E) dimethyl dihydrogenated tallow (Me2HT), and (F) tetradecyltrimethylol bis(3-mercaptopropionate)dimethylammonium bromide (trithiol).

having functionalities equal to or greater than three are recommended.[40] Unfortunately, such monomer systems tend to have high viscosities producing difficult processing conditions.

Synergistically combining the potential for improved physical properties derived from incorporating clay nanoparticles with the unique properties of thiol−ene photopolymers could lead to new and improved photopolymer nanocomposites. This goal may be realized through development of a fundamental understanding of the influence of organoclay on the photopolymerization behavior. Previous studies have shown no significant changes in polymerization behavior when organoclays are incorporated into the nanocomposite systems.[11] Others have also shown that modifying clay surfaces with polymerizable moieties induces significantly different polymerization behavior and mechanical properties. The resulting properties are often dependent on the type of reactive functionality utilized.[22] By considering the potential mechanical and thermal property improvement attainable with reactive organoclays, photopolymer systems with improved polymerization behavior and unique properties could be developed.[41]

This study investigates the influence of organoclay on the photopolymerization behavior as well as on thermal, mechanical, and shrinkage properties of nanocomposite systems based on thiol−acrylate monomer systems. The photopolymerization behavior of organoclay modified with typical quaternary ammonium surfactants was investigated. The study was extended to examine the effects of acrylated or thiolated organoclays on nanocomposite properties and photopolymerization behavior. Additionally, changes in mechanical properties and polymerization-induced shrinkage are probed to understand the evolution of nanocomposite properties as a function of photopolymerization behavior.

Experimental Section

Materials. To examine the influence of polymerizable organoclay nanoparticles on the photopolymerization behavior of thiol−acrylate formulations, tripropylene glycol diacrylate, (TrPGDA, Sartomer, Exton, PA) and trimethylolpropane tris(3-mercaptopropionate) (TMPTMP, Aldrich) were used. Polymerizable organoclays were developed by exchanging sodium cations on Cloisite Na (Southern Clay Products, Gonzalez, TX) with acrylate and thiol-modified quaternary ammonium surfactants. Cloisite Na has a cation exchange capacity (CEC) of 92.6 mequiv/100 g. Tetradecyl-2-acryloyloxy(ethyl)dimethylammonium bromide (C14A) and octadecyl-2-acryloyloxy(ethyl)dimethylammonium bromide (C18A) are acrylated quaternary ammonium surfactants synthesized following previously described methodologies.[42] Organoclays bearing these surfactants were produced following standard cation exchange procedures.[43] Thiol-modified clay (trithiol−organoclay) was synthesized by coupling a multifunctional thiol monomer to C14A-modified clay through a Michael addition reaction scheme following previously reported procedures.[41] Cloisite 15A (CL15A), an organically modified clay having no polymerizable functionality, was used for comparison. Cloisite 15A is modified with quaternary ammonium salt of dihydrogenated tallow (dihydrogenated consists of ~65% C18, ~30% C16, and ~5% C14 aliphatic chains, CEC = 125 mequiv/100 g). Figure 1 shows the chemical structures of monomers and surfactants used in this study. Ethyl alcohol (EA; Aaper Alcohol and Chemical, Shelbyville, KY), tetrahydrofuran (THF; Aldrich), and diethylamine (DEA; Aldrich) were used as received to synthesize trithiol−organoclay. 2,2-dimethoxyphenylacetophenone (DMPA; Ciba) was used as the free radical photoinitiator in all polymerizations at 0.1 wt %. A 1:1 molar mixture of TrPGDA and TMPTMP based on monomer functionality was used as the base monomer composition in all experiments. Since thiols do not homopolymerize significantly, the equimolar concentration was chosen to ensure reaction of the thiol monomers in the formulation. Even at 100% of the cation exchange capacity, molar concentration of acrylate or thiol functional groups on the organoclay surface is much less than the bulk monomer and was considered negligible. Table 1 summarizes typical compositions of formulations used in this experiment. For brevity, all organoclays will be referred to by the type of surfactant followed by organoclay, e.g., C14A−organoclay to reference C14A surfactant-modified clay.

Methods. *Photopolymerization Kinetics.* Samples for photopolymerization and viscoelastic property measurements were prepared by adding requisite amounts of organoclay to TrGPDA and sonicating for 2 h. Photoinitiator was added to the organoclay mixture and allowed to dissolve over a minimum 2 h period. TMPTMP was then added, and the sample was vortexed to form a uniform mixture. Photopolymerization behavior was monitored using real-time infrared spectroscopy (RTIR; Thermo Nicolet Nexus

Table 1. Composition of Samples Used in Experiments

organoclay	percent organoclay	mass of organoclay (g)	mass of TrPGDA (g)	moles of TrPGDA[a]	mass of TMPTMP (g)	moles of TMPTMP[a]	mass of photoinitiator (g)	total sample mass (g)
Cloisite 15A	0	0.00	1.21	3.53×10^{-3}	0.99	2.36×10^{-3}	2.00×10^{-3}	2
	1	0.02	1.19	3.49×10^{-3}	0.98	2.33×10^{-3}	2.00×10^{-3}	2
	3	0.07	1.16	3.41×10^{-3}	0.95	2.27×10^{-3}	2.00×10^{-3}	2
	5	0.12	1.14	3.32×10^{-3}	0.93	2.22×10^{-3}	2.00×10^{-3}	2
C14A−organoclay	1	0.03	1.19	3.49×10^{-3}	0.97	2.32×10^{-3}	2.00×10^{-3}	2
	3	0.08	1.16	3.39×10^{-3}	0.95	2.26×10^{-3}	2.00×10^{-3}	2
	5	0.13	1.13	3.30×10^{-3}	0.92	2.20×10^{-3}	2.00×10^{-3}	2
C18A−organoclay	1	0.03	1.19	3.48×10^{-3}	0.97	2.32×10^{-3}	2.00×10^{-3}	2
	3	0.09	1.15	3.38×10^{-3}	0.95	2.25×10^{-3}	2.00×10^{-3}	2
	5	0.14	1.12	3.28×10^{-3}	0.92	2.19×10^{-3}	2.00×10^{-3}	2
trithiol−organoclay	1	0.03	1.19	3.48×10^{-3}	0.97	2.32×10^{-3}	2.00×10^{-3}	2
	3	0.09	1.15	3.38×10^{-3}	0.95	2.25×10^{-3}	2.00×10^{-3}	2
	5	0.14	1.12	3.28×10^{-3}	0.92	2.19×10^{-3}	2.00×10^{-3}	2

[a] TrPGDA functionality = 2, TMPTMP functionality = 3. Moles of TrPGDA and TMPTMP are adjusted to achieve equal moles of functional groups when acrylated or thiolated organoclay is added to the formulation.

670).[44] RTIR samples were prepared by sandwiching 25 μL samples between two sodium chloride slides. The samples were purged with dry nitrogen gas for ~6 min before initiating polymerization. Aftereffects studies[45,46] were conducted by illuminating samples to a desired conversion, shuttering the light source, and monitoring functional group conversion in the "dark". These reactions were initiated with a 365 nm light at 3 mW/cm^2.

Mechanical Properties. To determine viscoelastic properties, rectangular bars measuring approximately 2 × 13 × 25 mm were fabricated by irradiating samples sandwiched between two microscope slides that were end-capped with 2 mm spacers. The monomers were purged for 10 min and irradiated for 10 min on each side. Before mechanical testing, all samples were stored at room temperature for at least 48 h. Young's modulus measurements were taken at 30 °C with an applied dynamic tensile force in the linear regime (typically less than 5% strain) and 1 Hz frequency using dynamic mechanic analysis (DMA; Q800 DMA TA Instruments). Data shown are averages of at least three runs.

Shrinkage Measurement. Polymerization-induced shrinkage properties were measured on a Physica MCR301 rheometer (Anton Paar) equipped with UV cell and H-PTD200 hood for temperature control and nitrogen atmosphere. Shrinkage was measured from samples sandwiched between 25 mm parallel plates. Systems were irradiated with a 100 W mercury short arc lamp and a bandpass filter that transmits only 320−500 nm wavelengths (Omnicure 1000-EXFO). The end of the light guide was fitted with a neutral density filter to control light intensity during experiments (Edmund Optics). The bottom plate in the rheometer was glass, and all experiments were performed under nitrogen purge. Photorheometer experiments were carried out using 1% oscillatory strain and a frequency of 1 Hz. An initial gap was set to 0.7 mm. Because of low starting viscosity, samples were loaded by lowering the top plate to the specified gap and then injecting samples to fill the gap. Shrinkage was measured by setting the instrument to maintain the force normal to the shear direction at 0 N. As the samples shrank, the gap was thus reduced to maintain a 0 N force, and shrinkage was recorded as change in gap vs time. In each experiment, the shutter was opened after 16 s, and the sample was continuously irradiated for the rest of the experiment with an intensity of 0.8 mW/cm^2.

Results and Discussion

Photopolymerization Behavior of Nonreactive Organoclay Systems. Previous research has shown that the rate of photopolymerization of acrylate-based systems generally decreases when nonpolymerizable organoclay is added. In particular, the maximum rate of photopolymerization decreases with increasing organoclay concentration in the photopolymerization of acrylate monomers.[22] In thiol−acrylate systems which polymerize by a combination of both chain and step-growth mechanisms, little is known regarding the effects of inorganic particle and their surface functionality on polymerization behavior, especially in clay−photopolymer systems. Lee et al. demonstrated that lower photopolymerization rates occur when small concentrations (up to 5 wt %) of thiol-functionalized spherical silica nanoparticles are incorporated into a thiol−acrylate formulation.[47] The reduced rate was attributed to surface effects and species concentration imbalance at the silica−monomer interface. To understand if similar photopolymerization behavior is observed with platelike particles, RTIR was used to monitor the photopolymerization behavior of thiol−acrylate systems containing organoclay.

A relatively low-viscosity monomer mixture comprising 1:1 molar ratio of difunctional acrylate (TrPGDA) and trifunctional thiol (TMPTMP) was investigated. Equimolar concentrations of acrylate and thiol monomers were used since the thiol monomer does not homopolymerize. Parts a and b of Figure 2 show acrylate and thiol functional group conversion plots as a function of time, respectively. Without thiol monomer or organoclay in the formulation, TrPGDA initially polymerizes slowly and accelerates (due to the Tromsdorff effect) to a final conversion of ~80% after 1 min of illumination. The rate of photopolymerization and final double-bond conversion changes significantly upon adding TMPTMP to the acrylate monomer. The observed autoacceleration effect in photopolymerizing TrPGDA is enhanced in the thiol−acrylate mixture. First, the rate of acrylate photopolymerization increases substantially in the TrPGDA/TMPTMP copolymer system. In addition, acrylate conversion increases to greater than 95%. This behavior is likely due to a more loosely cross-linked TrPGDA/TMPTMP polymer network, which now consists of a mixture of acrylate homopolymers and thiol−acrylate copolymers. The step growth nature of the thiol−acrylate reaction delays vitrification and could allow greater free radical mobility to yield the higher conversion. When 1 wt % CL15A, a nonpolymerizable organoclay, is added to the TrPGDA/TMPTMP sample, the initial slope of the acrylate conversion curve appears similar to that for the pure monomer mixture. Nearly complete double-bond conversion is also observed in the same period as the unfilled formulation. Upon the addition of 3 or 5 wt % CL15A, however, somewhat decreased double-bond conversion occurs, although the polymerization rates remain similar to the samples containing 1 wt % organoclay.

Thiol functional group conversion for these polymerizations follows similar trends as the acrylate conversions. Thus, after 1 min of illumination, thiol functional groups in the unfilled mixture reach ~60% conversion. Slightly lower thiol conversion is observed when 1 wt % CL15A is added to the monomer mixture. The overall conversion increases with higher organoclay concentration. However, the final conversion of formulations that have up to 5 wt % CL15A remains lower than the unfilled system. Overall, the maximum thiol conversion reaches between 50 and 60% when up to 5 wt % of CL15A is added.

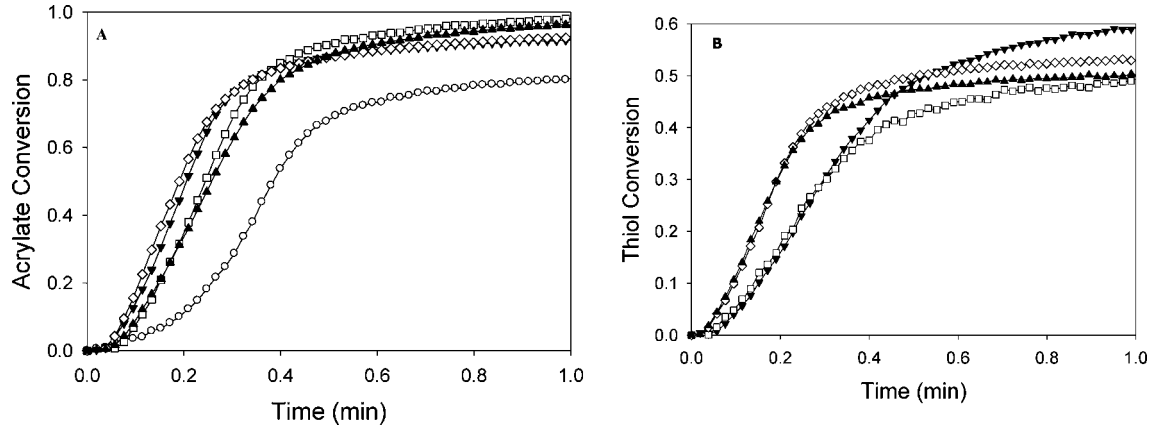

Figure 2. RTIR conversion profiles of Cloisite 15A in 1:1 mol (based on functional groups) TrPGDA/TMPTMP mixture. Shown are (A) acrylate double-bond conversion for TrPGDA (○), TrPGDA/TMPTMP (▼), and TrPGDA/TMPTMP with 1 wt % (□), 3 wt % (◇), and 5 wt % (▲) Cloisite 15A. (B) Thiol functional group conversion for TrPGDA/TMPTMP (▼) and TrPGDA/TMPTMP with 1 wt % (□), 3 wt % (◇), and 5 wt % (▲) Cloisite 15A.

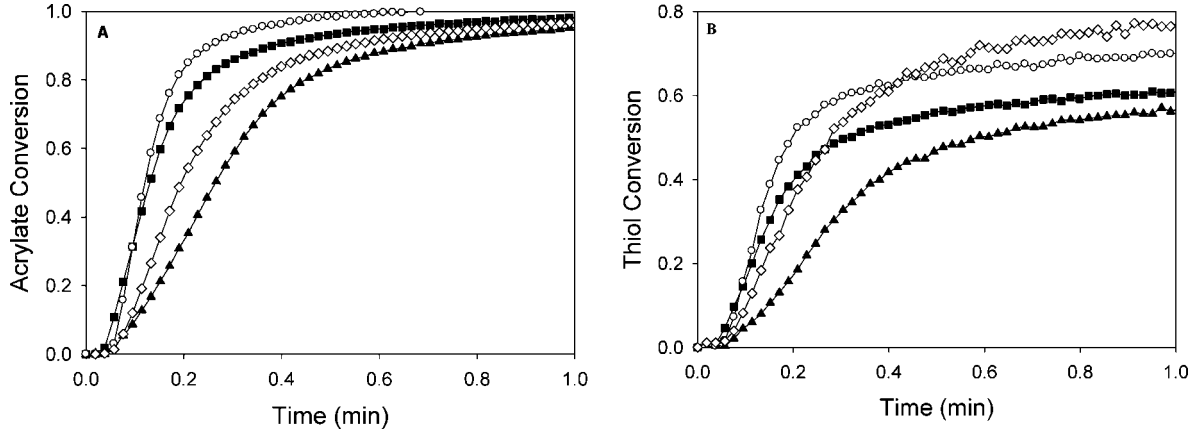

Figure 3. Plot of functional group conversions for (A) double-bond conversion vs time for TrPGDA/TMPTMP with 0 wt % (▲), 1 wt % (■), 3 wt % (○), and 5 wt % (◇) C14A−organoclay in 1:1 mol (based on functional groups) TrPGDA/TMPTMP. (B) Conversion of thiol functional groups for TrPGDA/TMPTMP with 0 wt % (▲), 1 wt % (■), 3 wt % (○), and 5 wt % (◇) C14A−organoclay.

With 3 and 5 wt % CL15A, the polymerization rate of the thiols appears to increase slightly as indicated by the greater slope of the conversion curve. Even with small changes in acrylate and thiol conversion and rates, the organoclay does not appear to influence the polymerization behavior of the thiol−acrylate mixture significantly. This behavior is in sharp contrast to that of pure acrylate systems in which increasing nonpolymerizable organoclay concentration often lowers the photopolymerization rates.[22]

Photopolymerization Behavior of Polymerizable Organoclay Systems. Introducing reactive functional groups onto the clay surface could allow much different photopolymerization behavior of the thiol−acrylate system in similar fashion as observed in other photopolymerizable systems. Previous work has shown that modification of clay surfaces with reactive groups enhances photopolymerization rates relative to nonreactive organoclay analogues.[22] Therefore, the polymerization kinetics were studied for TrPGDA/TMPTMP samples containing organoclays that have been modified with polymerizable functional groups. C14A−organoclay has acrylate functional groups that are capable of reacting with either TrPGDA or TMPTMP monomer. Trithiol−organoclay, on the other hand, is modified with thiol groups that can only copolymerize with the TrPGDA monomer.

The effects of C14A−organoclay on the photopolymerization behavior were investigated via RTIR. Parts a and b of Figure 3 show conversion profiles of acrylate and thiol functional groups as a function of time, respectively. The plots of acrylate conversion appear significantly different from that observed in systems with CL15A. Adding between 1 and 5 wt % C14A−organoclay to the monomer mixture leads to slightly higher double-bond conversion. Essentially 100% functional group conversion is observed when up to 5 wt % organoclay is incorporated into the monomer. In addition, the rate of photopolymerization is altered significantly compared to the CL15A system. Incorporation of 1 wt % C14A−organoclay leads to substantially higher photopolymerization rates compared to the unfilled TrPGDA/TMPTMP mixture and translates into shorter times to reach complete double-bond conversion. Further increases in photopolymerization rates are observed when 3 wt % C14A−organoclay is added to the formulation. With 5 wt % organoclay loading, the rate does decrease compared to either the 1 or 3 wt % organoclay systems. However, adding C14A−organoclay at all concentration levels investigated leads to photopolymerization rates that are substantially higher than the unfilled monomer mixture. Both the rate of polymerization and double-bond conversion behavior is in direct contrast to the observed behavior in nonpolymerizable organoclay system in which similar polymerization rates and lower conversions are observed with higher organoclay content.

The extent of thiol conversion also exhibits significant changes in comparison to the unfilled monomer mixture. Compared to the unfilled system, a slight increase in thiol conversion is observed when 1 wt % C14A−organoclay is

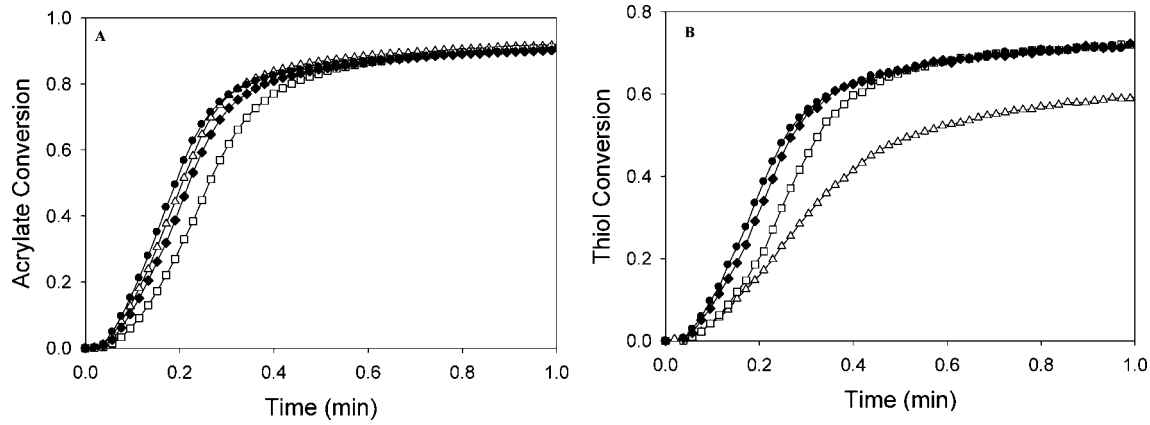

Figure 4. Conversion profiles of trithiol−organoclay in 1:1 mol (based on functional groups) TrPGDA/TMPTMP. (A) Acrylate conversion for neat TrPGDA/TMPTMP (Δ) and TrPGDA/TMPTMP with 1 wt % (□), 3 wt % (◆), and 5 wt % (●) trithiol−organoclay. (B) Thiol functional group conversion for neat TrPGDA/TMPTMP (Δ) and TrPGDA/TMPTMP with 1 wt % (□), 3 wt % (◆), and 5 wt % (●) trithiol−organoclay.

added. At 3 wt % C14A−organoclay loading, close to 70% thiol conversion is observed. A further increase in conversion (to ∼80%) occurs when 5 wt % C14A−organoclay is added to the formulation (Figure 3b). The rate of thiol conversion also appears to be greater when the polymerizable organoclay is incorporated into the monomer mixture. Unlike the nonpolymerizable organoclay system, adding the reactive functionality leads to faster photopolymerization rate and higher thiol monomer conversion.

Addition of thiol functionality onto clay surface provides another window through which the influence of organoclay surface functionality on thiol−acrylate polymerization behavior can be understood. Thiol polymerization requires addition of species with terminal double bonds with which to copolymerize.[39] Therefore, reaction of thiol species on the organoclay surface is dependent on the presence of acrylate monomer in the clay galleries. To examine the reaction behavior of these thiol−organoclay systems, C14A−organoclay was modified with multifunctional thiol monomer through a Michael addition reaction.[41] Trithiol−organoclay concentrations of up to 5 wt % organoclay were dispersed in an equimolar mixture of TrPGDA/TMPTMP monomer (equal moles of functional groups). Figure 4 shows RTIR conversion vs time plots for 1−5 wt % trithiol−organoclay in TrPGDA/TMPTMP. Approximately 90% double-bond conversion is observed upon adding the organoclay. Ultimate functional group conversions in the trithiol−organoclay formulations were independent of organoclay concentration. Similar rates of photopolymerization are observed for all concentrations of thiol−organoclay after 1 min of illumination. Interestingly, addition of thiol−organoclay leads to similar acrylate photopolymerization behavior as observed in the nonpolymerizable organoclay systems.

Thiol conversion in the trithiol−organoclay samples, however, differs from the samples containing either CL15A or C14A−organoclay. Approximately 70% of thiol species is converted when 1−5 wt % trithiol−organoclay is added to the mixture. Figure 4b shows that the conversion is independent of organoclay concentration since similar final conversions are observed for up to 5 wt % concentration. While more thiol monomer convert into the polymer matrix compared to the CL15A system at any concentration level, it is interesting to note that trithiol−organoclay does not induce significant concentration-dependent behavior. However, samples containing trithiol−organoclay polymerize faster than the neat formulation. Increasing the organoclay concentration to 3 or 5 wt % leads to slightly faster polymerization rates relative to the 1 wt % sample and even higher in comparison to the neat sample.

Surface Interaction Effects. Clearly, the photopolymerization behavior appears to be influenced significantly by the type of functionality incorporated into the organoclay. To further understand the mechanism for the observed photopolymerization behavior upon introducing organoclay into the reaction mixture, after-effects experiments were performed.[45,46] After-effects studies are conducted by shuttering the initiation light source at various double-bond conversions. With no exposure to light, the initiation rate goes to zero. Therefore, any observed reaction is directly related to the nature of radicals remaining in the system. Functional group conversion determined in the dark can then be correlated to free radical longevity and concentration. Better understanding of the mechanism for the observed changes in photopolymerization behavior can be gained from monitoring such "dark" reactions.

Real-time infrared spectroscopy measurement of dark conversion as a function of conversion during illumination is shown in Figure 5. Postillumination acrylate and thiol conversions for TrPGDA/TMPTMP mixture containing 3 wt % organoclay are shown in parts a and b of Figure 5, respectively. Without organoclay, double-bond conversion in the mixture increases by ∼10% after illuminating the sample to ∼10% conversion. Irradiating the unfilled sample to higher conversion levels before shuttering the light leads to lower dark conversion as ∼6% dark cure occurs when irradiation is maintained to achieve 35% double-bond conversion. On the other hand, dark conversion of double bonds actually increases when the samples are polymerized to higher conversions before shuttering the light in the presence of CL15A. While 8% more acrylate functional groups polymerize in the dark for samples that are illuminated to 10% conversions, further 15% dark conversion occurs in samples that are illuminated to 35% conversion before shuttering the light. C14A−organoclay achieves almost double the dark conversion levels compared to the unfilled formulation or the other organoclay systems. Thus, nearly 20% additional acrylate conversion is observed in the C14A−organoclay systems at different shutter times and conversions. On the contrary, ∼10% dark conversion is observed in samples with trithiol−organoclay even after illuminating to achieve 40% conversion.

Dark conversion of thiol functional groups appear to behave in a similar manner as the acrylates. Thus, both the unfilled monomer and trithiol−organoclay samples have lower conversion levels in the dark when compared to the C14A−organoclay samples (Figure 5b). Approximately 6% thiol functional group conversion is observed in the dark for the unfilled formulation and samples that contain trithiol−organoclay. In comparison, substantially higher dark conversion (∼14%) occurs in the C14A−organoclay samples under the same polymerization

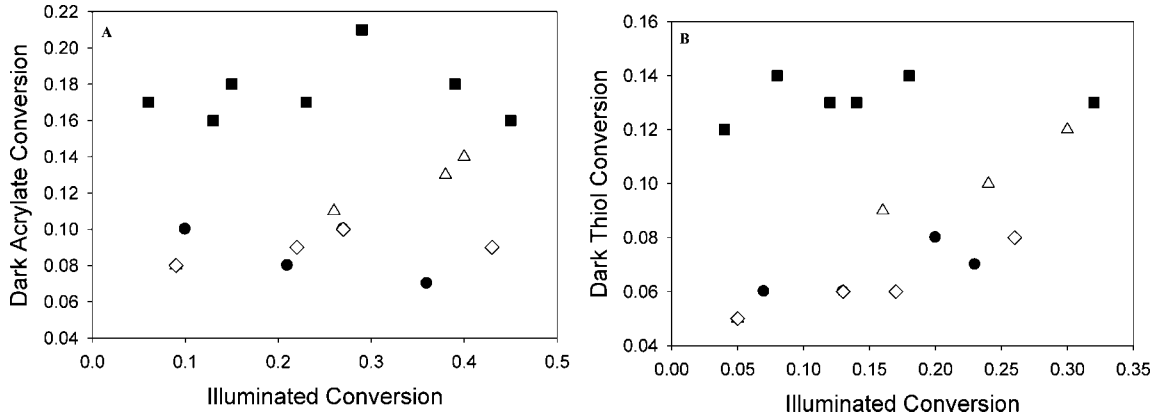

Figure 5. Dark conversion of thiol−acrylate formulations: (A) double-bond conversion in the dark vs conversion during irradiation of 1:1 mol (based on functional groups) TrPGDA/TMPTMP (●) and TrPGDA/TMPTMP with 3 wt % Cloisite 15A (Δ), 3 wt % C14A−organoclay (■), and 3 wt % trithiol−organoclay (◇). (B) Thiol functional group conversion for TrPGDA/TMPTMP (●) and TrPGDA/TMPTMP with 3 wt % Cloisite 15A (Δ), 3 wt % C14A−organoclay (■), and 3 wt % trithiol−organoclay (◇).

conditions. CL15A and the unfilled samples initially have similar dark conversions for illuminated conversions up to 15%. Dark conversion increases as the samples are illuminated to higher conversions before shuttering the light. Since no more free radicals are generated after shuttering the initiating light source, the behavior observed in Figure 5 suggests that free radical concentration depends on the added organoclay. The number of free radicals generated in C14A−organoclay is the highest among the four samples. The free radicals also appear longer lived and suggest a change to the polymerization mechanism upon introducing acrylated organoclay into the reaction medium.

Considering the low concentration of C14A surfactants on the clay surface, the higher free radical concentration in C14A−organoclay sample is likely not due to increased double-bonds concentration. More likely, this behavior may be attributed to decreased termination rates as indicated by the higher conversion and polymerization rates. In terms of the photopolymerization behavior, immobilizing free radicals on the clay surface leads to faster polymerization rates due to diffusion limitations. Because of their immobility, growing radical chains from the polymerizable species on the clay surface are less likely to participate in bimolecular termination, resulting in the observed behavior in Figure 5. In addition, the free radicals could polymerize rapidly with other acrylate species along the surface due to the close proximity of adjacent molecules anchored on the particle surface. Hence, the clay surface may serve as a medium for facilitating faster polymerization rates in a similar fashion as observed in other templated polymerizations.[24,25] For free radicals generated from C14A molecules on the clay surface, such a mechanism is consistent with what has been observed previously in pure acrylate−organoclay systems.[22] This additional radical propagation and polymerization would also lead to the higher overall thiol and acrylate conversions in the presence of C14A−organoclay. On the contrary, the lack of such propagation mechanism in the CL15A formulations is evident in the lower thiol functional group conversion as well as slower rates of conversion.

To gain further understanding of the differences in polymerization of both thiolated and acrylated organoclay systems, polymerization behavior in the early stages of the reaction was examined more closely. RTIR plots of double-bond vs thiol conversion in the first 15 s of reaction are shown in Figure 6 for samples containing 3 wt % organoclay and the neat monomer mixture. The graph indicates that illuminating the unfilled monomer mixture for 15 s leads to ∼45% double-bond and 18% thiol conversion. For this system, double bonds are converted at more than twice the rate of thiols. Acrylate conversion in the C14A−organoclay system reaches almost 50% for 15% thiol

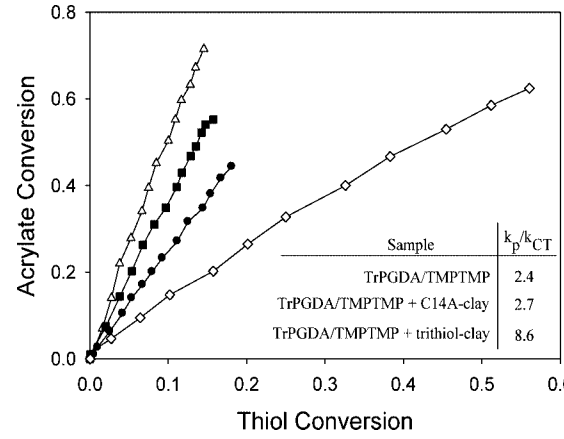

Figure 6. Double-bond vs thiol conversion at short irradiation times for 1:1 mol (based on functional groups) TrPGDA/TMPTMP (●), TrPGDA/TMPTMP with 3 wt % Cloisite 15A (Δ), 3 wt % C14A−organoclay (■), and 3 wt % trithiol−organoclay (◇). Samples were irradiated for 15 s using 365 nm light at 3 mW/cm^2.

conversion. In comparison, the thiol−organoclay system shows much different polymerization behavior from the other systems. At 20% double-bond conversion, ∼15% conversion of thiol functional groups is observed.

Previous studies have demonstrated that acrylate homopolymerization occurs extensively in acrylate/thiol mixtures.[48] Hence, the polymerization behavior of the TrPGDA/TMPTMP mixture and C14A−organoclay systems are consistent with typical acrylate−thiol copolymerizations. In the thiol−organoclay system, however, the similarity in double-bond and thiol functional group conversions suggests that acrylate−thiol copolymerization occurs to a more significant degree relative to the other formulations. The nature of the copolymerization observed is indicative of significant preference for a step-growth reaction behavior. Clearly, the nature of the organoclay functionality alters the polymerization behavior significantly and could have a significant impact on the properties of the resulting nanocomposite.

From the above discussions, the faster photopolymerization rates and higher functional group conversions (both acrylate and thiol) could further be explained considering the nature of acrylate or thiol polymerization at the organoclay−monomer interface. It has been shown previously that acrylate homopolymerization in a thiol−acrylate system occurs at a faster rate compared to the copolymerization.[34] For the C14A−organoclay system, rapid polymerization of free radicals along the surface

due to templating effects could lead to the observed photopolymerization behavior. In addition, immobilization of free radical chains would lead to lower termination rates and, ultimately, faster polymerizations as observed. On the other hand, because thiol molecules at the clay surface do not hompolymerize, potentially faster polymerization induced by immobilizing species on the particle surface could depend on the concentration of acrylate monomer within the clay galleries. Upon reacting anchored thiol molecules with acrylate radicals, polymerization can ensue between either thiol or acrylate monomers in the gallery. Consequently, rapid polymerization along the surface would occur only after the surfactant molecule reacts with a homopolymerizable species. This may also allow copolymerization that approaches a true alternating reaction in the bulk.

In preparing samples, C14A−organoclay mixes uniformly with TrPGDA, while trithiol−organoclay and CL15A phase separate over time from TrPGDA. Upon adding thiol monomer, CL15A still exhibits some phase separation while the trithiol−organoclay forms uniform mixtures. The observed mixing properties suggest that the acrylate monomer tends to swell C14A−organoclay to a greater degree than either the CL15A or trithiol−organoclay. Such swelling would lead to higher initial intragallery acrylate monomer concentration in the C14A−organoclay system, while a mixture of thiol and acrylate monomers would induce trithiol−organoclay swelling. Hence, at the organoclay−monomer interface, acrylate homopolymerization proceeds rapidly due to decreased termination from immobilizing C14A radicals as well as potentially higher localized monomer concentrations. Since acrylate homopolymerization is more rapid in thiol−acrylate copolymerizations, the observed polymerization behavior strongly supports the faster reaction mechanism in the C14A−organoclay system. For the thiol−organoclay system, the tendency to induce swelling by a mixture of thiol and acrylate monomers may lead to relatively lower intragallery acrylate concentration. Since the thiol−acrylate copolymerization is slower, the overall polymerization rate would be reduced as compared to the sample containing C14A−organoclay.

Polymerization Rate Parameters. To understand further the influence of the type of reactive organoclay on the observed polymerization dynamics, apparent propagation and chain transfer rate parameters were evaluated according to eq 1.[48] The apparent chain propagation rate (k_p) and chain transfer rate (k_{CT}) parameters were calculated using eq 1:

$$\frac{d[C{=}C]}{d[SH]} = 1 + \frac{k_p}{k_{CT}}\frac{[C{=}C]}{[SH]} \quad (1)$$

where d[C═C] and d[SH] are the rates of acrylate and thiol polymerization, respectively, k_p represents apparent propagation rate parameter for acrylate homopolymerization, k_{CT} is the apparent chain transfer to thiol, [C═C] is molar concentration of acrylate, and [SH] represents thiol molar concentration. The rates of polymerization (d[C═C] and d[SH]) are deduced from the first derivative of conversion vs time plots from RTIR data.[45,46] Since conversion of functional groups versus time is known from the RTIR plots, [C═C] and [SH] is calculated as follows:

$$[C{=}C]_0(1 - x)_{C=C} \quad (2a)$$

$$[SH]_0(1 - x)_{SH} \quad (2b)$$

$$\frac{d[C{=}C]}{d[SH]} = 1 + \frac{k_p}{k_{CT}}\frac{[C{=}C]_0(1 - x)_{C=C}}{[SH]_0(1 - x)_{SH}} \quad (3)$$

where x is fraction conversion and $[SH]_0$ and $[C{=}C]_0$ are the initial molar concentrations of TMPTMP and TrPGDA, respectively. The limit as d[SH] approaches 0 in eq 3 is 1. Hence, a plot of d[C═C]/d[SH] vs [C═C]/[SH] in eq 3 with the vertical axis intercept set to 1 yields the value of k_p/k_{CT}. On the basis of experimental results for neat formulations as well as monomer mixtures containing 3 wt % organoclay, the apparent chain transfer rate parameter for trithiol−organoclay samples is 9 times less than the propagation rate parameter. For the C14A−organoclay samples, the apparent k_p/k_{CT} has a value of ∼3, while the unfilled mixture has an apparent k_{CT} that is ∼2 times less than the apparent k_p (see Figure 6 inset). This supports the greater degree of acrylate homopolymerization in samples containing C14A−organoclay and the tendency toward step-growth copolymerization behavior in the trithiol−organoclay system. Since the copolymerization step in thiol−acrylate mixtures is slower compared to acrylate homopolymerization, the trend toward copolymerization in trithiol−organoclay systems would lead to slower polymerization rates. Similarly, faster photopolymerization rates would be observed for the C14A−organoclay system because of the higher tendency of acrylate monomers to homopolymerize in that system.

Influence of Dispersant Chain Length. The ability to modulate the degree of copolymerization in binary thiol−acrylate formulations potentially has significant implications in the design of clay−photopolymer nanocomposite systems. For instance, modifying clay surfaces with the appropriate functionality could facilitate control of the polymerization mechanism, network structure, and thereby nanocomposite properties. Such techniques could be useful in optimizing dispersion behavior of organoclay in various polymer matrices. Considering that monomer diffusion into clay galleries and delamination induced by larger polymer chains may cause exfoliation,[49] changing the polymerization dynamics could be a useful tool in material design. For example, the greater degree of step growth behavior in thiolated organoclay systems could facilitate exfoliation due to delayed gelation during reaction, while acrylated organoclays could be utilized to increase thiol conversion in binary thiol−acrylate photopolymers.

Previous research has shown that chemical similarity of the dispersant and monomer can significantly alter ultimate clay morphology. To determine the effect of increasing the oleophilic nature, and thereby changing the compatibility of the polymerizable surfactant, a C14A analogue with longer aliphatic tail was developed. The effects of this increased aliphatic chain length on photopolymerization behavior were examined using octadecyl-2-acryloyloxy(ethyl)dimethylammonium bromide (C18A) surfactant to form C18A−organoclay. The influence of C18A−organoclay on photopolymerization kinetics of the TrPGDA/TMPTMP formulation was investigated via RTIR. Conversion profiles as a function of time for both acrylate and thiol functional groups in the TrPGDA/TMPTMP mixture containing C18A−organoclay are shown in parts a and b of Figure 7, respectively. Complete double-bond conversion is observed when 1 wt % C18A−organoclay is added to the TrPGDA/TMPTMP monomer mixture. Upon increasing the concentration of C18A−organoclay up to 5 wt %, the extent of double-bond conversion decreases to levels slightly above the neat monomer mixture. Additionally, lower polymerization rates occur when higher concentrations of organoclay are added to the monomer mixture. Similar photopolymerization rates occur when 3 and 5 wt % organoclay is added to the formulation, with both formulations exhibiting higher acrylate polymerization rates compared to the unfilled monomer.

Conversion of thiol monomers differs from the C14A−organoclay system in that the conversion behavior is apparently independent of organoclay concentration. Slightly more than 60% conversion is observed upon adding C18A−organoclay to the TrPGDA/TMPTMP mixture. In addition, similar thiol

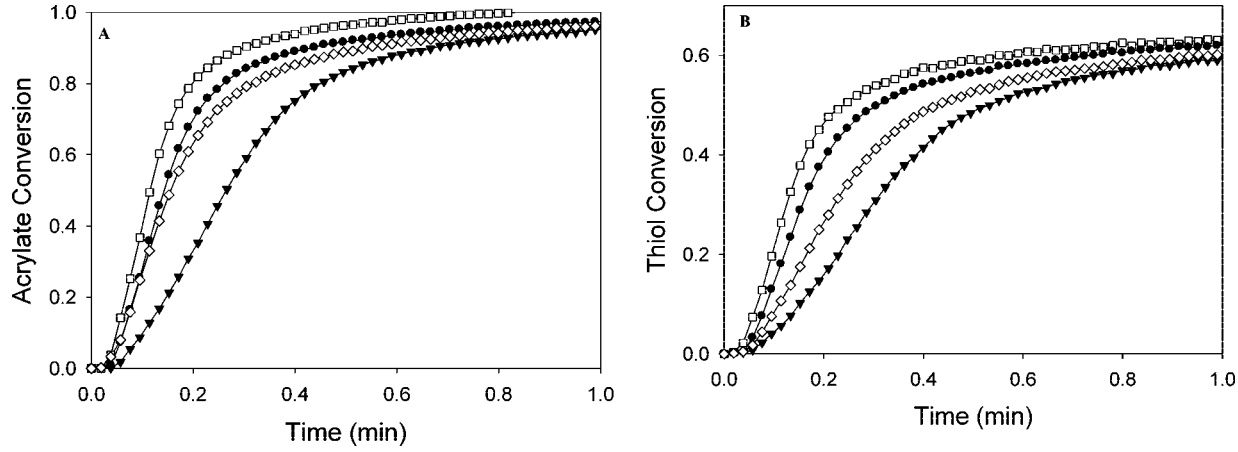

Figure 7. RTIR profiles for (A) double-bond conversion of 1:1 mol (based on functional groups) TrPGDA/TMPTMP (▼), TrPGDA/TMPTMP with 1 wt % (□), 3 wt % (●), and 5 wt % (◇) C18A−organoclay. (B) Thiol conversion for TrPGDA/TMPTMP (▼) and TrPGDA/TMPTMP with 1 wt % (□), 3 wt % (●), and 5 wt % (◇) C18A−organoclay.

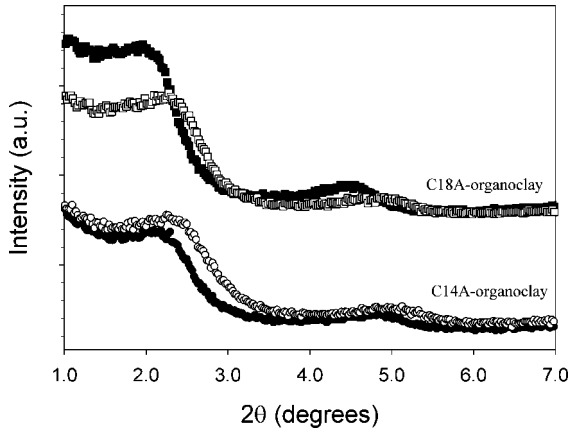

Figure 8. SAXS profiles of 3 wt % C14A−organoclay in TrPGDA/TMPTMP before polymerization (●) and after polymerization (○) and of 3 wt % C18A−organoclay in TrPGDA/TMPTMP before polymerization (■) and after polymerization (□).

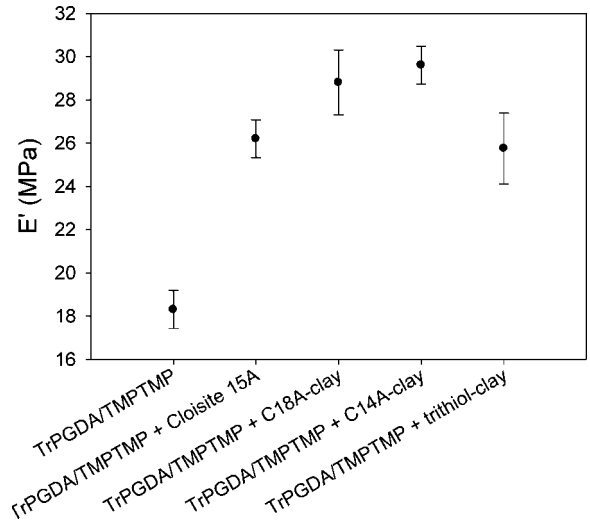

Figure 9. Young's modulus of 3 wt % organoclay in TrPGDA/TMPTMP. Data were taken at 30 °C using a frequency of 1 Hz.

levels are observed in both filled and unfilled formulations when C18A−organoclay is added. Unlike the C14A−organoclay, however, similar thiol conversion levels are observed for samples containing up to 5 wt % organoclay. The rate of thiol conversion changes when C18A−organoclay is added to the monomer mixture. Greater rates of thiol conversion as compared to the neat polymer are observed with organoclay addition. Incorporating higher concentrations of C18A−organoclay (from 1 to 5 wt %) results in corresponding increases in the rate of photopolymerization. Such thiol conversions observed in the C18A−organoclay system are interesting considering the conversion behavior in samples that contain C14A−organoclay. Since polymerization behavior may change due to aggregation of organoclay particles,[41] the dispersion of C18A−organoclay was examined to determine morphological changes in the clay aggregates.

Dispersion Behavior of Acrylated Organoclays. Accordingly, SAXS was used to characterize the dispersion behavior of the organoclays in the TrPGDA/TMPTMP monomer mixture. Figure 8 shows X-ray scattering profiles of 3 wt % C14A or C18A−organoclay in the TrPGDA/TMPTMP mixture. The position of the primary peaks in the SAXS profiles of both unpolymerized C14A−organoclay and C18A−organoclay samples show *d*-spacing of 4.5 and 4.6 nm, respectively. A peak shift to higher 2θ is observed in both organoclay systems after photopolymerization, indicating a reduction in *d*-spacing. Though diffused, the prominent peaks observed in the polymerized samples also indicate that both C14A− and C18A−organoclays form primarily intercalated domains in the polymer. Considering the differences in polymerization behavior, the similarity in dispersion behavior suggests that the aggregation of C18A molecules on the particle surface is significantly different from C14A dispersants. The longer aliphatic chains of C18A molecules could reduce accessibility to the surface acrylate functional groups through steric effects. Hence, fewer immobilized species are available for polymerization to the bulk monomers. This behavior could explain the lower thiol functional group conversion observed in C18A−organoclay samples as enhancement in conversion appears to be due to reaction through radicals on the clay surface.

Physical Properties. While significant advances have led to improvements in the properties of thiol−ene photopolymers, addition of organoclay to improve mechanical properties may be another alternative to further expand existing applications. In addition, the enhanced conversion and rate behavior observed could also be a useful tool for tailoring the physical properties of thiol−acrylate photopolymer systems. Mechanical properties were investigated by evaluating the elastic modulus of 3 wt % of the various organoclay in TrPGDA/TMPTMP polymer via dynamic mechanical analysis instrument. Figure 9 shows the Young's modulus as a function of the type of organoclay. Addition of 3 wt % CL15A increases the Young's modulus by

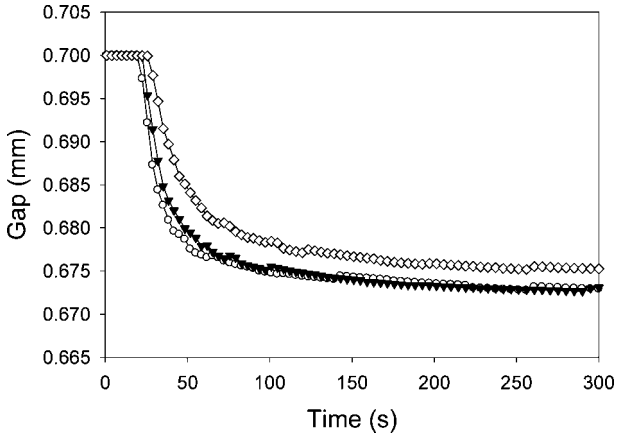

Figure 10. Volumetric shrinkage as measured by change in sample gap during photopolymerization. Samples contain 3 wt % Cloisite 15A (▼) or trithiol−organoclay (◇) dispersed in TrPGDA/TMPTMP. Neat polymerization of TrPGDA/TMPTMP (○) is also shown for comparison. Polymerizations were performed at 0.8 mW/cm^2.

~40% over the neat polymer. Incorporation of either C14A−organoclay or C18A−organoclay leads to even higher increases in modulus (ca. 50%) compared to the unfilled polymer while the Young's modulus is 40% higher than the neat polymer when the same amount of trithiol−organoclay is added. The higher modulus in the acrylated organoclay systems could be due to the higher functional group conversions. In the trithiol−organoclay system, the increased tendency toward a step growth mechanism, which leads to relatively lower cross-linked networks, results in the lower modulus. It is interesting to note that by changing the functionality of the polymerizable organoclay, the reaction behavior could be modulated to afford different network properties in these photopolymers.

In addition to polymerization behavior and mechanical properties, another physical property that affects the performance of nanocomposites was examined to elucidate the impact of organoclay on thiol−ene photopolymers. Polymerization-induced shrinkage, a major concern in applications of pure (meth)acrylate systems, is generally reduced in thiol−ene systems.[50] However, shrinkage reduction is typically achieved at the expense of mechanical properties since higher shrinkage is associated with increasing modulus. To investigate the influence of polymerizable organoclays on shrinkage in thiol−acrylate photopolymers, photorheometry studies were used to monitor polymerization-induced shrinkage of samples containing 3 wt % organoclay (Figure 10). These experiments were conducted at lower light intensity to more accurately capture the influence of the organoclays. Only results for CL15A and trithiol−organoclay compared to the neat polymer are presented for illustration. The sample gap decreases during polymerization by the same amount in both the neat polymer and CL15A samples while trithiol−organoclay samples show significantly less decrease in the gap length. This implies that similar degrees of volumetric shrinkage occur in the CL15A system as the unfilled polymer. The trithiol−organoclay system, however, exhibits lower volumetric shrinkage compared to either the unfilled polymer or the CL15A−organoclay system. Additionally, the onset of polymerization induced shrinkage appears to commence later than the nonpolymerizable organoclay system or the neat polymer. The lower degree of shrinkage as well as the delayed incidence of shrinkage is further evidence of the shift in reaction mechanism in the trithiol−organoclay system. Since the reaction mechanism in thiol−acrylate copolymerizations evolves more through a step-growth nature, formation of high molecular weight polymer networks occur more slowly. This behavior has been shown to relieve stresses through delayed gelation in such polymer systems and apparently results in low shrinkage in this system.[50]

Conclusions

The effects of adding organically modified clay nanoparticles bearing both thiol and acrylate functional groups on the polymerization, mechanical, and shrinkage properties of a thiol−acrylate system have been evaluated. Higher photopolymerization rates and conversions of both acrylate and thiol occur in acrylated organoclay systems compared to both unfilled thiol−acrylate mixtures. With thiols on the clay surface, little difference is observed in the rate of photopolymerization as organoclay concentration increases. Similarly, introducing a nonpolymerizable organoclay into TrPGDA/TMPTMP formulation does not change acrylate and thiol functional group conversion appreciably. The enhanced polymerization behavior with acrylated organoclay is related to reduced termination rates due to presence of immobilized radicals on the clay surface. Introducing thiol functionality into the organoclay changes the polymerization behavior toward a step-growth reaction mechanism in which both acrylate and thiol functionalities convert to similar degrees early in the reaction. This behavior increases thiol conversion to higher levels than the unfilled mixture. The thiolated organoclay system also exhibit thiol conversion behavior that is less dependent on organoclay concentration. Materials with higher modulus are generated as a result of the higher functional group conversions in the acrylated organoclay system. Additionally, adding thiolated organoclay reduces polymerization induced shrinkage in comparison to the neat photopolymer.

Acknowledgment. The authors acknowledge financial support from the National Science Foundation (CTS-0626395), the IUCRC Center for Fundamentals and Applications of Photopolymerization, an NSF-AGEP fellowship (University of Iowa), and a Department of Education GAANN fellowship. Dr. John Woods (Henkel Corp.) is also acknowledged for invaluable discussions and help with photorheometry experiments.

References and Notes

(1) Giannelis, E. P. *Adv. Mater.* **1996**, *8*, 29–35.
(2) LeBaron, P. C.; Wang, Z.; Pinnavaia, T. J. *Appl. Clay Sci.* **1999**, *15*, 11–29.
(3) Pindzola, B. A.; Jin, J.; Gin, D. L. *J. Am. Chem. Soc.* **2003**, *125*, 2940–2949.
(4) Bueeler, M.; Spoerl, E.; Seiler, T.; Mrochen, M. *Proc. SPIE* **2008**, *6844*(Ophthalmic Technologies XVIII), 68440Z/1−68440Z/11.
(5) Vermonden, T.; Fedorovich, N. E.; van Geemen, D.; Alblas, J.; van Nostrum, C. F.; Dhert, W. J. A.; Hennink, W. E. *Biomacromolecules* **2008**, *9*, 919–926.
(6) Mayo-Pedrosa, M.; Alvarez-Lorenzo, C.; Lacik, I.; Martinez-Pacheco, R.; Concheiro, A. *J. Pharm. Sci.* **2006**, *96*, 93–105.
(7) Mauguiere-Guyonnet, F.; Burget, D.; Fouassier, J. P. *Prog. Org. Coat.* **2006**, *57*, 23–32.
(8) Sangermano, M.; Malucelli, G.; Amerio, E.; Priola, A.; Billi, E.; Rizza, G. *Prog. Org. Coat.* **2005**, *54*, 134–138.
(9) Decker, C. *Polym. News* **2005**, *30*, 34–48.
(10) Roffey, C. G. *Photopolymerisation of Surface Coatings*; Wiley: New York, 1982.
(11) Decker, C.; Keller, L.; Zahouily, K.; Benfarhi, S. *Polymer* **2005**, *46*, 6640–6648.
(12) Uhl, F. M.; Davuluri, S. P.; Wong, S. C.; Webster, D. C. *Chem. Mater.* **2004**, *16*, 1135–1142.
(13) Uhl, F. M.; Webster, D. C.; Davuluri, S. P.; Wong, S.-C. *Eur. Polym. J.* **2006**, *42*, 2596–2605.
(14) Zahouily, K.; Benfarhi, S.; Bendaikha, T.; Baron, J.; Decker, C. *Proc. RadTech Europe* **2001**, 583.
(15) Decker, C.; Zahouily, K.; Keller, L.; Benfarhi, S.; Bendaikha, T.; Baron, J. *Proc. RadTech North America* **2002**, *309*, 320.
(16) Decker, C. *Polym. Nanocompos.* **2006**, *188*, 205.
(17) Decker, C.; Zahouily, K.; Keller, L.; Benfarhi, S.; Bendaikha, T.; Baron, J. *J. Mater. Sci.* **2002**, *37*, 4831–4838.

(18) Benfarhi, S.; Decker, C.; Keller, L.; Zahouily, K. *Eur. Polym. J.* **2004**, *40*, 493–501.
(19) Wang, Y.-Y.; Hsieh, T.-E. *J. Mater. Sci.* **2007**, *42*, 4451–4460.
(20) Hailin, T.; Nie, J. *Macromol. React. Eng.* **2007**, *1*, 384–390.
(21) Landry, V.; Riedl, B.; Blanchet, P. *Prog. Org. Coat.* **2008**, *62*, 400–408.
(22) Owusu-Adom, K.; Guymon, C. A. *Polymer* **2008**, *49*, 2636–2643.
(23) Polowinski, S. *Prog. Polym. Sci.* **2002**, *27*, 537–577.
(24) Clapper, J. D.; Sievens, L.; Guymon, C. A. *Chem. Mater.* **2008**, *20*, 768–781.
(25) Clapper, J. D.; Guymon, C. A. *Adv. Mater.* **2006**, *18*, 1575–1580.
(26) Decker, C. *Polym. Int.* **1998**, *45*, 133–141.
(27) Decker, C. *Prog. Polym. Sci.* **1996**, *21*, 593–650.
(28) Hoyle, C. E.; Lee, T. Y.; Roper, T. *J. Polym. Sci., Part A: Polym. Chem.* **2004**, *42*, 5301–5338.
(29) Li, Q.; Zhou, H.; Wicks, D. A.; Hoyle, C. E. *J. Polym. Sci., Part A: Polym. Chem.* **2007**, *45*, 5103–5111.
(30) Wei, H.; Li, Q.; Ojelade, M.; Madbouly, S.; Otaigbe, J. U.; Hoyle, C. E. *Macromolecules* **2007**, *40*, 8788–8793.
(31) Senyurt, A. F.; Wei, H.; Hoyle, C. E.; Piland, S. G.; Gould, T. E. *Macromolecules* **2007**, *40*, 4901–4909.
(32) Reddy, S. K.; Okay, O.; Bowman, C. N. *Macromolecules* **2006**, *39*, 8832–8843.
(33) Rydholm, A. E.; Reddy, S. K.; Anseth, K. S.; Bowman, C. N. *Biomacromolecules* **2006**, *7*, 2827–2836.
(34) Lee, T. Y.; Bowman, C. N. *Polymer* **2006**, *47*, 6057–6065.
(35) Lu, H.; Carioscia, J. A.; Stansbury, J. W.; Bowman, C. N. *Dent. Mater.* **2005**, *21*, 1129–1136.
(36) Cramer, N. B.; Reddy, S. K.; Lu, H.; Cross, T.; Raj, R.; Bowman, C. N. *J. Polym. Sci., Part A: Polym. Chem.* **2004**, *42*, 1752–1757.
(37) Lee, T. Y.; Smith, Z.; Reddy, S. K.; Cramer, N. B.; Bowman, C. N. *Macromolecules* **2007**, *40*, 1466–1472.
(38) Lee, T. Y.; Carioscia, J.; Smith, Z.; Bowman, C. N. *Macromolecules* **2007**, *40*, 1473–1479.
(39) Morgan, C. R.; Magnota, F.; Ketley, A. D. *J. Polym. Sci., Polym. Chem. Ed.* **1977**, *15*, 627–645.
(40) Hoyle, C. E.; Cole, M.; Bachemin, M.: Kuang, W.; Kalyanaraman, V.; Jonsson, S. In *Photoinitiated Polymerizations*, ACS Symposium Series 847; Belfield, K. D., Crivello, J. V., Eds.; American Chemical Society: Washington, DC, 2003; p 52.
(41) Owusu-Adom, K.; Guymon, C. A., manuscript accepted in *Macromolecules*.
(42) Hamid, S. M.; Sherrington, D. C. *Polymer* **1987**, *28*, 325–331.
(43) Katti, K. S.; Sikdar, D.; Katti, D. R.; Ghosh, P.; Verma, D. *Polymer* **2006**, *47*, 403–414.
(44) Decker, C.; Moussa, K. *J. Coat. Technol.* **1990**, *62*, 55–61.
(45) Anseth, K. S.; Wang, C. M.; Bowman, C. N. *Macromolecules* **1994**, *27*, 650–655.
(46) Tryson, G. R.; Shultz, A. R. *J. Polym. Sci., Polym. Chem. Ed.* **1979**, *17*, 2059–2075.
(47) Lee, T. Y.; Bowman, C. N. *Polymer* **2006**, *47*, 6057–6065.
(48) Lecamp, L.; Houllier, F.; Youssef, B.; Bunel, C. *Polymer* **2001**, *42*, 2727–2736.
(49) Bousmina, M. *Macromolecules* **2006**, *39*, 4259–4263.
(50) Jacobine, A. T. In *Polymerization Mechanisms*; Fouassier, J. P., Rabek, J., Eds.; Science Publishers Ltd.: New York, 1993; pp 219−268.

MA802656X